LAWRENCE
LIVERMORE
NATIONAL
LABORATORY

LLNL-JRNL-470580

Structural and electronic properties of dense liquid and amorphous nitrogen

B. Boates, S. A. Bonev

February 15, 2011

Physical Review B

Disclaimer

Structural and electronic properties of dense liquid and amorphous nitrogen

Brian Boates[1,2] and Stanimir A. Bonev[1,2]
[1] *Lawrence Livermore National Laboratory, Livermore, CA 94551, USA and*
[2] *Department of Physics, Dalhousie University, Halifax, NS B3H 3J5, Canada*
(Dated: February 10, 2011)

We present first-principles calculations of the structural and electronic properties of liquid nitrogen in the pressure-temperature range of 0-200 GPa and 2000-6000 K. The molecular-polymerization and molecular-atomic liquid phase boundaries have been mapped over this region. We find the polymeric liquid to be metallic, similar to what has been reported for the higher-temperature atomic fluid. An explanation of the electronic properties is given based on the structure and bonding character of the transformed liquids. We discuss the structural and bonding differences between the polymeric liquid and insulating solid cubic-gauche nitrogen to explain the differences in their electronic properties. Furthermore, we discuss the mechanism responsible for charge transport in polymeric nitrogen systems to explain the conductivity of the polymeric fluid and the semi-conducting nature of low-temperature amorphous nitrogen.

PACS numbers: 62.50.-p,02.70.-c, 61.20.Ja,31.15.at,73.61.Jc

I. INTRODUCTION

The behavior of molecular solids and liquids under extreme conditions is of fundamental interest in the field of condensed matter physics and chemistry. At high pressures (P) and temperatures (T) these materials often undergo dissociation and/or polymerization transitions to new phases with interesting properties[1,2]. In particular, polymeric nitrogen has become a subject of intense research in recent years. If meta-stable under ambient conditions, polymeric nitrogen could be important as a high-energy-density material. At pressures near and above 100 GPa molecular nitrogen was found to transform into a narrow-gap ($\sim$ 0.6 eV) semi-conducting amorphous phase (η-N)[3–6]. Extrapolation of experimental band gap energies suggests η-N becomes metallic above 300 GPa at room temperature[5]. Above 2000 K at comparable pressures, nitrogen forms the insulating single-bonded cubic-gauche phase (cg-N). This phase was predicted[7] over a decade before its experimental verification[1]. Recently, there have been many studies on the thermodynamic stability of other polymeric crystalline phases of nitrogen, with some possessing lower enthalpy than cg-N at higher pressures, though none have been observed experimentally[8–17].

Previous shock-wave experiments have shown that molecular liquid nitrogen undergoes a continuos transformation to a conducting atomic liquid at high-P and T[18–20]. Subsequent first-principles calculations[21,22] also reported molecular dissociation and metallization in good agreement with experiment. In both studies, the authors emphasize the correlation between the fraction of dissociated atoms and the electrical conductivity as it is states attributed to the dissociated atoms that begin to populate the dense liquid band gap.

At lower temperatures it was predicted that the molecular liquid undergoes a first-order phase transition to a polymeric liquid upon compression[23]. The structure of the emerging liquid continues to evolve with pressure; upon transformation, the liquid is predominantly 2-coordinated while further compression yields more 3-coordinated atoms. The band gap was found to close upon transformation to the polymeric liquid, indicating that the molecular-polymeric transition may coincide with an insulator-metal transition[24].

In this paper, we report the results of first-principles calculations on the structural and electronic properties of liquid nitrogen. The frequency dependent conductivity $\sigma(\omega)$, and reflectivity $R(\omega)$, of liquid nitrogen have been calculated. We find the polymeric liquid to be metallic in contrast to the known insulating polymeric solid cg-N and provide an explanation for this difference based on differences in the structure and bonding of the two phases. An analogy is made between the polymeric liquid and the low-temperature semi-conducting amorphous solid based on compelling similarities in their structure. The mechanism responsible for electronic transport in polymeric nitrogen is presented and used to explain the differences in the electronic properties of the two disordered polymeric phases.

II. COMPUTATIONAL METHOD

A. First-principles molecular dynamics

First principles molecular dynamics (FPMD) simulations of nitrogen have been performed for pressures up to 200 GPa and temperatures up to 6000 K using finite-temperature density functional theory (DFT)[25] within the Perdew-Burke-Ernzerhof generalized gradient approximation (PBE-GGA)[26] as implemented in $VASP$[27]. The FPMD simulations were carried out in the canonical (NVT) ensemble using Born-Oppenheimer dynamics and a Nosé-Hoover thermostat. Simulations were equilibrated within 1-2 ps and continued for over 10 ps using a 0.75 and 0.50 fs ionic time-step. Simulations were performed with 64 and 128-atom supercells, a 5-electron

projector augmented wave (PAW) pseudopotential with a 1.50 Bohr core radius, and a 500 eV plane-wave cut-off. Changes in E, P, and structure were negligible when checked using a PAW pseudopotential with a 1.10 Bohr core radius with a 944.5 eV plane-wave cut-off.

Further convergence studies of **k**-point sampling and finite-size effects were carried out over a wide range of P-T conditions: before and after polymerization and dissociation, as well as at the highest-pressures considered. These included: (i) FPMD simulations with 64-atom supercells and a $2 \times 2 \times 2$ **k**-point grid; and (ii) static calculations with a $2 \times 2 \times 2$ and $4 \times 4 \times 4$ **k**-point grid on 128-atom FPMD configurations. In all cases, changes in E, P, and the structure were well within the error-bars.

To validate our methods we have calculated the P-V equation of state (EOS) of cg-N at finite-temperature in good agreement with experimental data[28,29] which was shown in our previous work[23]. Vibrational frequencies in our simulated molecular fluid also compare well with experimental results[30] near 50 GPa and 2000 K. Furthermore, our simulations suggest the onset of molecular dissociation above 30 GPa at 6000 K in excellent agreement with previous experimental[20] and theoretical work[22].

B. Electronic properties

The electronic conductivity was evaluated for several densities along the 2000, 3000, and 6000 K isotherms. At each density considered, the conductivity was averaged over 10-30 well-spaced configurations from a 64-atom FPMD trajectory. The occupation of the orbitals was determined based on a Fermi-Dirac distribution with an electronic temperature equal to the ionic temperature. We have used a 5-electron PAW pseudopotential with a 1.11 Bohr core radius and a 40 Ha plane-wave cut-off within PBE-GGA DFT in *abinit*[31,32]. We used a $4\times4\times4$ **k**-point grid for calculations of 64-atom cells. The real part of the frequency-dependent conductivity was evaluated using the Kubo-Greenwood formalism[33,34]:

$$\sigma_1(\omega) = \frac{2\pi e^2\hbar^2}{3m^2\omega\Omega}\sum_{\mathbf{k}} W(\mathbf{k}) \sum_{j=1}^{N}\sum_{i=1}^{N}\sum_{\alpha=1}^{3}[F(\epsilon_{i,\mathbf{k}}) - F(\epsilon_{j,\mathbf{k}})] \times|\langle\Psi_{j,\mathbf{k}}|\nabla_\alpha|\Psi_{i,\mathbf{k}}\rangle|^2\delta(\epsilon_{i,\mathbf{k}} - \epsilon_{j,\mathbf{k}} - \hbar\omega), \quad (1)$$

where m and e are the mass and charge of an electron, Ω is the cell volume, α is an index over cartesian directions, and $F(\epsilon_{i,\mathbf{k}})$ represents the occupation of the i'th eigenvalue at **k**-point **k**. The zero-frequency limit of this expression yields the direct current (DC) conductivity σ_{DC}. The imaginary part of the frequency-dependent conductivity is given by the Kramers-Krönig transform:

$$\sigma_2(\omega) = -\frac{2}{\pi}P\int_0^\infty \frac{\sigma(\nu)\omega}{(\nu^2-\omega^2)}d\nu \quad (2)$$

where the principal value of the integral is given by P. The complex dielectric function ϵ, index of refraction n, coefficient of extinction k, and reflectivity R can be obtained using the complex conductivity:

$$\epsilon_1(\omega) = 1 - \frac{4\pi}{\omega}\sigma_2(\omega) \quad ; \quad \epsilon_2(\omega) = \frac{4\pi}{\omega}\sigma(\omega) \quad (3)$$

$$\epsilon(\omega) = \epsilon_1(\omega) + i\epsilon_2(\omega) = [n(\omega) + ik(\omega)]^2 \quad (4)$$

$$R(\omega) = \frac{[1-n(\omega)]^2 + k^2(\omega)}{[1+n(\omega)]^2 + k^2(\omega)} \quad (5)$$

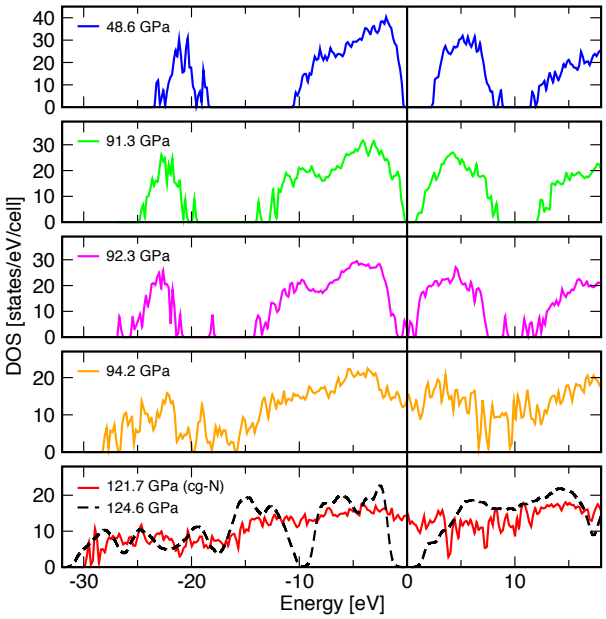

FIG. 1. Electronic density of states of liquid nitrogen at 3000 K and insulating cg-N at 2000 K. States begin to populate the band gap as the molecular liquid transforms into the polymeric liquid phase, before closing the gap entirely over a very small pressure range. At 3000 K the liquid-liquid transition occurs at 92 GPa.

III. RESULTS

A. Electronic properties

The electronic density of states (DOS) of liquid nitrogen is shown in Fig. 1 for several densities along the 3000 K isotherm. At low pressure the liquid is molecular and insulating with a GGA band gap near 2 eV. The DOS at 2000 K of the known single-bonded insulating solid phase, cg-N, is also shown for comparison. Upon compression the DOS remains relatively unchanged until approaching the polymerization transition. As the triple bonded molecules begin to destabilize, new polymeric compounds are formed and the band gap closes rapidly with pressure. Thus, the liquid polymerization transition coincides with an insulator-metal transition.

Fig. 2 shows the frequency-dependent conductivity of liquid nitrogen along the 3000 K isotherm. The low-density molecular liquid possesses two distinct peaks

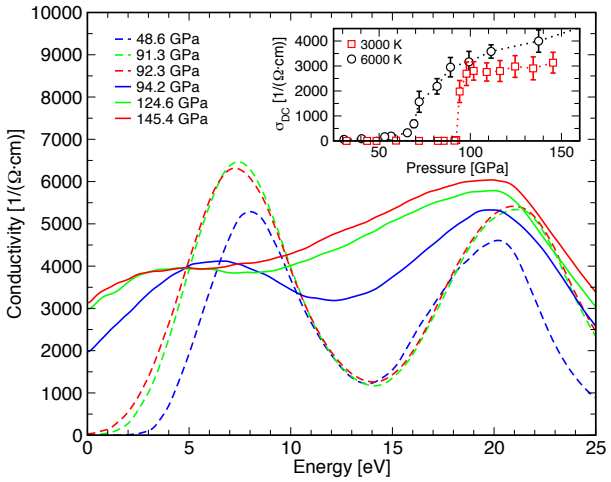

FIG. 2. Frequency dependent conductivity of liquid nitrogen along the 3000 K isotherm. (inset) DC conductivity as a function of pressure along the 3000 and 6000 K isotherms.

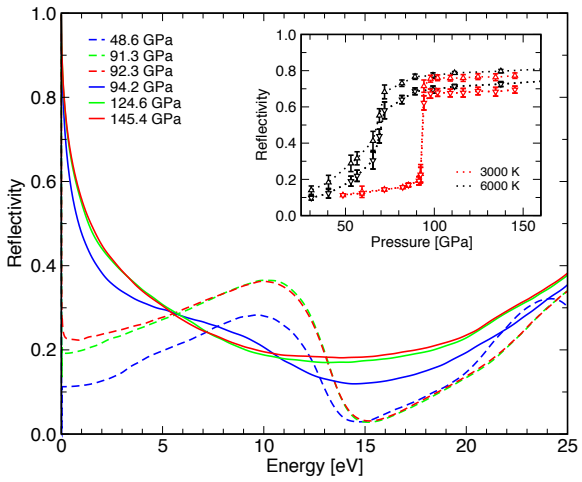

FIG. 3. Frequency dependent reflectivity of liquid nitrogen along the 3000 K isotherm. (inset) Reflectivity at 532 (downward triangles) and 1064 nm (upward triangles) as a function of pressure for 3000 (red) and 6000 K (black) isotherms.

which gradually disappear with increasing pressure. Most notable is the jump in DC conductivity upon reaching the liquid phase boundary near 92 GPa. The inset shows the DC conductivity as a function of pressure along the 3000 K isotherm. The DC conductivity is zero at low pressures as the fluid is purely molecular. At the liquid-liquid phase boundary, the DC conductivity sharply increases to a nearly constant value of 3000 $(\Omega\cdot\mathrm{cm})^{-1}$. A similar increase is also found in σ_{DC} along the 6000 K isotherm, consistent with previous calculations of dissociating liquid nitrogen along the 5000 K isotherm[22]. Note the gradual increase in the conductivity as the molecules dissociate compared to the discontinuous increase when they undergo polymerization. This is related to the gradual nature of the high-T dissociation transition of nitrogen molecules, whereas the lower-T polymerization is first-order.

We have also computed the frequency dependent reflectivity along the 3000 isotherm, shown in Fig. 3. The reflectivity curves show a progression similar to what we find in the computed conductivities. As the reflectivity is a common experimental observable, we provide its pressure dependence at 3000 and 6000 K for wavelengths of 532 and 1064 nm. The reflectivities at these wavelengths increase sharply at the 3000 K polymerization phase boundary and plateau to a value near 0.70. The reflectivities for these wavelengths are also shown for comparison at 6000 K, which show a gradual increase with pressure before plateauing to comparable values. Measurement of the conductivity and reflectivity may prove useful in the experimental detection of the polymeric fluid and in future measurements of the high-pressure melting curve.

B. Relation to structural properties

At low pressure the insulating nature of molecular liquid nitrogen can simply be explained by the electrons being strongly localized within the triple bond. At very high temperatures the molecular bonds destabilize upon compression and begin to dissociate into a metallic atomic phase. In the atomic liquid, the system becomes metallic as a result of dopant dissociated atoms filling the band gap. At lower temperatures the breaking of molecules leads to the formation of covalently bonded polymeric compounds rather than dissociated atoms. Although covalent bonding is still present in the polymeric liquid, it too is metallic. Moreover, the known polymeric cg-N phase is an insulator, while the low-T amorphous η-N phase is semi-conducting. Thus, there must be significant differences in the electronic structure of the different polymeric phases which lead to large differences in their optical properties.

To relate the structure of polymeric nitrogen with the behavior observed in its electronic properties, we consider the atomic coordination of the different phases. The atomic coordination is defined as the number of atoms surrounding a given atom within a selected cut-off distance. As covalent bonding occurs in the first-peak regime of the pair correlation function $g(r)$, we have chosen our cut-off as the first minimum in $g(r)$. Fig. 4 (top) shows the DC conductivity of liquid nitrogen at 2000, 3000, and 6000 K. Amorphous and chain-like solids obtained through freezing of the high-P liquid at 2000 K are also shown. The fraction of 2-coordinated nitrogen atoms in each phase is given for direct comparison in Fig. 4 (bottom). The DC conductivity is zero for the low-P molecular liquid at 2000, 3000, and 6000 K, which coincides with the purely 1-coordinated

nature of the atoms. Upon compression, the liquid transforms into the polymeric phase at similar pressures for both 2000 and 3000 K. This leads to an increase in the fraction of 2-coordinated atoms in the system to approximately 75 and 60% at 2000 and 3000 K, respectfully. The increase in 2-coordinated atoms is accompanied by a qualitatively identical increase in σ_{DC} to approximately 3000 $(\Omega{\cdot}\mathrm{cm})^{-1}$, which remains relatively constant under further compression. The constant behavior of σ_{DC} is reflected in the fraction of 2-coordinated atoms and can also be explained by the constant nearest-neighbor bond length of 1.27 Åat these pressures. At 6000 K, the liquid undergoes a continuous molecular dissociation; we find that the resulting dissociated high-T fluid is also predominantly 2-coordinated. The important structural difference between the atomic fluid and polymeric fluid is therefore the dynamic stability of 2-coordinated nitrogen compounds, not simply their static presence. Thus, the conductivity in the atomic fluid can also be attributed to the presence of short-lived 2-coordinated compounds, similar to the polymeric case. Moreover, if one considers the aforementioned chain-like and amorphous solid phases obtained through FPMD freezing of the 2000 K liquid, one also finds a strong correlation between the 2-coordinated fraction and σ_{DC}. Almost all atoms in the chain-like phase are 2-coordinated resulting in a heightened DC conductivity. The high-T amorphous solid shares similar structural characteristics with the polymeric liquid, but possesses a slightly lowered conductivity, which may provide insight into the semi-conducting nature of the η-N phase. Lastly, entirely single-bonded (3-coordinated) cg-N is shown to illustrate how polymeric nitrogen without 2-coordinated atoms results in zero DC conductivity. Thus, phases that are purely 1-coordinated (molecular) and 3-coordinated (cg-N) exhibit no DC conductivity. The DC conductivity is only nonzero when 2-coordinated atoms are present, the amount of which is strongly correlated with the value of σ_{DC}. It is important to note that the mechanisms responsible for conductivity in the atomic and polymeric fluids are both directly tied to the presence of 2-coordinated nitrogen atoms, which fill the band gap. Conductivity resulting from electrons traveling along 2-coordinated nitrogen chain-like compounds is analogous to what is known for carbon hydrides such as trans-polyacetylene.

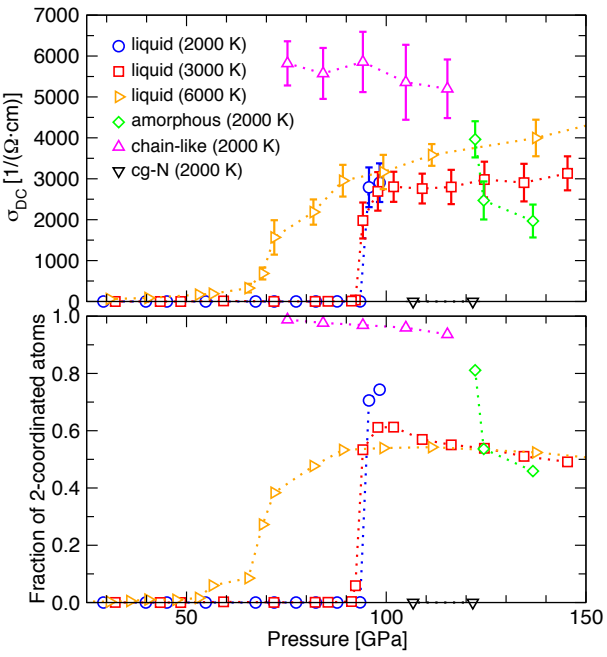

FIG. 4. (top) DC conductivity as a function of pressure for the 2000 K liquid (circles), 3000 K liquid (squares), 6000 K liquid (right triangles), 2000 K chain-like solid (upward triangles), 2000 K amorphous solid (diamonds), and cg-N at 2000 K (downward triangles). (bottom) Fraction of 2-coordinated atoms in each corresponding phase.

C. Amorphous nitrogen

Conducting polymers have been a subject of intense research for several years[35]. The prototypical example of a one-dimensional (1D) conducting polymer is trans-polyacetylene (trans-PA). The idealized structure of trans-PA can be described as a chain of equally spaced CH groups. In this configuration trans-PA would be a 1D metal as each carbon atom would supply one electron to a subsequently half filled π band. However, at low temperatures trans-PA undergoes a Peierls distortion, leading to a chain of alternating single and double bonded CH groups. This opens a gap at the Fermi level, making trans-PA a semi-conductor rather than a metal. The resulting experimental[36] (theoretical[37]) band gap and bond length alternation (BLA) are 1.5 eV (1.3 eV) and 0.08 Å (0.074 Å), respectively. The BLA is a common parameter used to describe Peierls distortions and is simply the difference in lengths of the bonds between neighboring atoms[36]. To describe the electronic properties of trans-PA, the so-called SSH Hamiltonian was written assuming that the local electronic density can be coupled to the length of the covalent bonds between carbon atoms along the chain and that the electronic structure of the π bands can be described with a tight-binding approximation as,

$$t_{n+1,n} = t_0 - \alpha(u_{n+1} - u_n), \tag{6}$$

$$H_{SSH} = \sum_{n,\sigma} -t_{n+1,n}(c^{\dagger}_{n+1,\sigma}c_{n,\sigma} + c^{\dagger}_{n,\sigma}c_{n+1,\sigma}) + \sum_{n}\left[\frac{p_n^2}{2m} + \frac{1}{2}K_n(u_{n+1} - u_n)^2\right]. \tag{7}$$

Where $t_{n+1,n}$ is the hopping integral to first-order, t_0 is the hopping integral for the equidistant chain, α is the electron-phonon coupling constant, u_n is the displacement of the n^{th} CH group along the axis of the chain

from equilibrium, $c^{\dagger}_{n,\sigma}$ and $c_{n,\sigma}$ are the creation and annihilation operator for π electrons on the n^{th} CH group, p_n are the nuclear momenta, m is the atomic mass of carbon, and K_n is an effective spring constant. The second sum in (7) describes the kinetic energy of the ions as well as the potential energy arising from the displacement of CH groups along the chain. In (6) it is assumed that the effects of a Peierls distortion are sufficiently small and can be approximated linearly.

We now argue that the chains of nitrogen atoms observed in the polymeric liquid and amorphous phases are both structurally and electronically analogous to trans-PA, where CH groups are replaced by single nitrogen atoms. Electronically, the hydrogen atoms in trans-PA are replaced by lone pairs in the case of nitrogen. Should the two cases be similar, one should observe similar Peierls-like distortions in an idealized chain of nitrogen atoms. This effect can be captured using hybrid functional techniques, as has been done for trans-PA[37]. To illustrate this effect in chain-like nitrogen compounds we have incorporated a mixture of Hartree-Fock (HF) exchange into our DFT calculations with the PBE0 hybrid functional in $VASP$[38]. We have performed calculations on an isolated prototypical 2-atom chain monomer found in polymeric liquid and amorphous nitrogen. We perform structural relaxations using a fixed cell: 10 Å for a and b lattice constants perpendicular to the direction of chain and 1.90 Å for c, parallel to the chain. A value of 10 Å for both a and b proved sufficient to avoid interaction with periodic replicas. A range of values from 1.70 to 2.20 Å were considered for c, the lattice constant responsible for the compression of the chain length. A value of 1.90 Å was chosen for this study as it gave bond lengths comparable to the dense liquid and amorphous phases; a different choice of c does not lead to qualitative differences. It is interesting to note that the magnitude of the Peierls distortion varies for different choices of c. Specifically, the size of the distortion tends to decrease for smaller values of c (*i.e.* as the chain length is compressed). This signifies that under compression, the system becomes more metallic as the distortion is reduced, consistent with measurements suggesting metallization of semi-conducting amorphous nitrogen upon further compression[5]. In terms of the SSH Hamiltonian description presented above, this corresponds to an increase in the effective spring constant K_n with compression, leading to a larger energy penalty with respect to chain distortions.

Structural relaxations using the hybrid functional led to large Peierls distortions, giving values for the bond length alternation (BLA) as high as 0.068 Å compared to 0.005 Å when not including any hybrid exchange. The prescribed amount of exact exchange to incorporate into a DFT calculation using the PBE0 functional is 25%, based on a comparison of atomization energies computed using fourth-order Moller-Plesset perturbation theory with the G1 test set[39]. However, small changes in the amount of mixing leads to large quantitative differences in the BLA and band gap of our system. Fig. 5 shows our results for the BLA and band gap of a single chain of nitrogen atoms for different fractions of hybrid mixing. Fig. 5 (a) illustrates how the size of the Peierls distortion is strongly dependent on the amount of exact exchange, as expected. Furthermore, Fig. 5 (b) shows the band gap resulting from each structural relaxation. We have computed the band gap of the resulting distorted chains using both hybrid and regular PBE functionals. It is clear that the use of hybrid exchange enhances the Peierls distortion, which opens the band gap. The band gap of the hybrid distorted chains were calculated using the respective amount of HF exchange (orange dashed) as well as with regular PBE (orange solid). The band gap of the PBE optimized chain was also calculated with various amounts of hybrid mixing (blue dashed). Fig 5 (c) shows the electronic band structure of optimized nitrogen chains using both PBE and hybrid (25% HF) functionals. It is clear that structural optimization using hybrid functionals opens a gap in the band structure, whether computed using hybrid or regular PBE functionals; this is of course related to the large Peierls distortion one achieves when employs a hybrid functional in structural optimizations. Moreover, the band gap of the regular PBE optimized chain is significantly larger when computed using hybrid functionals. The band structures of Peierls distorted chains of nitrogen atoms was previously investigated theoretically in the work of Pohl *etal.*[40]. They find a Peierls-like distortion using a local-density approximation (LDA) exchange-correlation functional, which we could not reproduce in this work. However, the band

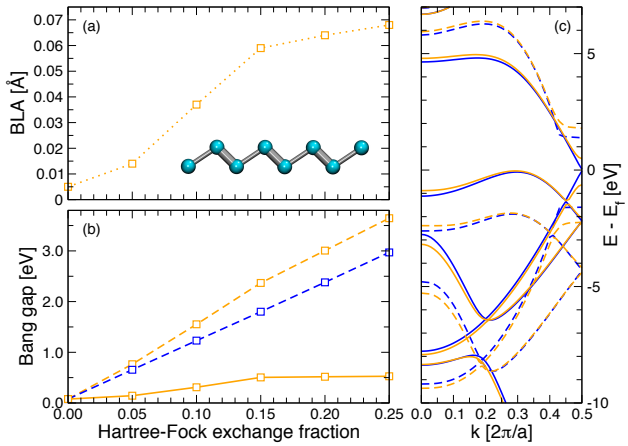

FIG. 5. (a): Bond length alternation (BLA) of a single nitrogen chain with respect to the amount of Hartree-Fock exchange mixing (as described in the text). (b) and (c): Resulting band gaps and electronic band structures of Peierls distorted chains using hybrid and regular PBE functionals. In both (b) and (c), calculations using a PBE (hybrid) functional for structural optimizations are shown in blue (orange); calculations of electronic properties using a PBE (hybrid) functional are given by solid (dashed) lines. A visualization of the Peierls distorted nitrogen chain is shown in (a).

structures they report for the distorted chain are similar to what we show in Fig. 5 (c). The notable difference between the electronic bands in polymeric nitrogen and aforementioned trans-PA is the presence of a relatively flat band located just below the Fermi level. This is attributed to the lone pairs in the nitrogen system compared to the CH σ bonds in trans-PA. It is important to note that although near the Fermi level, this band likely does not participate in electrical conductivity as the electrons are localized and have a large effective mass. This band is also found to drop significantly in energy when calculated using hybrid functionals.

We predict that the conducting behavior along chains of nitrogen atoms can be equivalently described by (7) and that the polymeric liquid and amorphous solid are characterized by these types of compounds. Thus, we propose that the polymeric liquid metal is a high temperature manifestation of the low-T semi-conducting amorphous η-N. In the polymeric liquid the Peierls distortions along the chains become negligible in comparison with the large ionic motion induced by the high temperatures allowing it to remain metallic. However, at lower temperatures, Peierls effects play a significant role in the electronic properties and lead to the semi-conducting state of η-N.

Furthermore, the Goldhammer-Herzfeld (GH) criterion for metallization has been used to provide upper bounds on the density one should expect metallization to occur due to ionization of the electrons[41] based on the gas phase polarizability. The GH densities for molecular and atomic nitrogen correspond to pressures of approximately 509 and 223 GPa, respectively, at 300 K. These pressures were obtained by fitting and extrapolating the P-V EOS obtained from FPMD simulations of amorphous nitrogen.

We have performed FPMD simulations of amorphous nitrogen by quenching the high-density liquid to lower temperatures. The structural analysis of the FPMD trajectories show that η-N is composed of a mixture of both 2 and 3-coordinated atoms, consistent with previous experimental work suggesting an average coordination of 2.5(3)[3].

There have been several measurements of the band gap of η-N characterizing it as a narrow gap semi-conductor with reported values for the gap near 0.6 eV above 150 GPa[3–5]. The band gap was found to decrease upon further compression, with an extrapolation that suggests metallization at pressures near 300 GPa[5], well above the GH metallization estimate for atomic nitrogen. We have computed the DOS of amorphous nitrogen over the range of pressures from 90-330 GPa. Although we find a substantial decrease in electronic states at the Fermi level, our calculations do not show a band gap opening for any of the pressures considered. Peierls distortions can be easily missed or largely underestimated with DFT[36], which could explain why we do not find a band gap in our calculations. If one wishes to apply hybrid techniques to calculations of η-N we propose calibrating the appropriate mixture of exact exchange using quantum Monte Carlo calculations. If done correctly, one should be able to accurately describe the optical properties of amorphous nitrogen.

IV. CONCLUSIONS

In summary, we find that the first-order polymerization transition reported in liquid nitrogen coincides with an insulator-metal transition similar to what has been observed for molecular dissociation at higher temperatures. The metallic behavior in the atomic and polymeric fluids is strongly correlated with the amount of 2-coordinated atoms present. We predict a DC conductivity for the polymeric liquid of approximately 3000 $(\Omega\cdot\mathrm{cm})^{-1}$, close to that of dissociated liquid nitrogen. Our results provide routes for experimental identification of the polymeric liquid through conductivity and reflectivity measurements. This may be particularly useful in the determination of the high-pressure melting curve of nitrogen. Furthermore, we describe the mechanism responsible for the semi-conducting behavior of amorphous nitrogen as a Peierls distortion and propose a method to accurately compute its optical properties.

V. ACKNOWLEDGMENTS

This work was performed under the auspices of the U.S. Department of Energy (DOE) at the University of California/LLNL under Contract No. DE-AC52-07NA27344. The authors acknowledge support from NSERC, Killam Trusts, and Acenet.

[1] M. I. Eremets, A. G. Gavriliuk, I. A. Trojan, D. A. Dzivenko, and R. Boehler, Nature Materials, **3**, 558 (2004).
[2] V. Iota, C. Yoo, and H. Cynn, Science, **283**, 1510 (1999).
[3] A. F. Goncharov, E. Gregoryanz, H. Mao, Z. Liu, and R. J. Hemley, Phys. Rev. Lett., **85**, 1262 (2000).
[4] M. I. Eremets, R. J. Hemley, H. Mao, and E. Gregoryanz, Nature, **411**, 170 (2001).
[5] E. Gregoryanz, A. F. Goncharov, R. J. Hemley, and H. Mao, Phys. Rev. B, **64**, 052103 (2001).
[6] M. J. Lipp, J. P. Klepeis, B. J. Baer, H. Cynn, W. J. Evans, V. Iota, and C. Yoo, Phys. Rev. B, **76**, 014113 (2007).
[7] C. Mailhiot, L. H. Yang, and A. K. McMahan, Phys. Rev. B, **46**, 14419 (1992).
[8] M. M. G. Alemany and J. L. Martins, Phys. Rev. B, **68**, 024110 (2003).

[9] W. D. Mattson, D. Sanchez-Portal, S. Chiesa, and R. M. Martin, Phys. Rev. Lett., **93**, 125501 (2004).
[10] F. Zahariev, A. Hu, J. Hooper, and T. Woo, Phys. Rev. B, **72**, 214108 (2005).
[11] H. L. Y. ad G. W. Yang, X. H. Yan, Y. Xiao, Y. L. Mao, Y. R. Yang, and M. X. Cheng, Phys. Rev. B, **73**, 012101 (2006).
[12] X. Wang, Z. He, Y. M. Ma, T. Cui, Z. M. Liu, B. Liu, J. F. Li, and G. T. Zou, J. Phys.: Condens. Matter, **19**, 425226 (2007).
[13] Y. Yao, J. S. Tse, and K. Tanaka, Phys. Rev. B, **77**, 052103 (2008).
[14] J. Kotakoski and K. Albe, Phys. Rev. B, **77**, 144109 (2008).
[15] C. J. Pickard and R. J. Needs, Phys. Rev. Lett., **102**, 125702 (2009).
[16] Y. Ma, A. R. Oganov, Z. Li, Y. Xie, and J. Kotakoski, Phys. Rev. Lett., **102**, 065501 (2009).
[17] X. Wang, F. Tian, L. Wang, T. Cui, B. Liu, and G. Zou, J. Chem. Phys., **132**, 024502 (2010).
[18] W. J. Nellis, N. C. Holmes, A. C. Mitchell, and M. van Thiel, Phys. Rev. Lett., **53**, 1661 (1984).
[19] H. B. Radousky, W. J. Nellis, M. Ross, D. C. Hamilton, and A. C. Mitchell, Phys. Rev. Lett., **57**, 2419 (1986).
[20] W. J. Nellis, H. B. Radousky, D. C. Hamilton, A. C. Mitchell, N. C. Holmes, K. B. Christianson, and M. van Thiel, J. Chem. Phys., **94**, 2244 (1991).
[21] S. Mazevet, J. D. Johnson, J. D. Kress, L. A. Collins, and P. Blottiau, Phys. Rev. B, **65**, 014204 (2001).
[22] S. Mazevet, J. D. Kress, L. A. Collins, and P. Blottiau, Phys. Rev. B, **67**, 054201 (2003).
[23] B. Boates and S. A. Bonev, Phys. Rev. Lett., **102**, 015701 (2009).
[24] D. Donadio, L. Spanu, I. Duchemin, F. Gygi, and G. Galli, Phys. Rev. B, **82**, 020102 (2010).
[25] W. Kohn and L. Sham, Phys. Rev., **140**, A1133 (1965).
[26] J. Perdew, K. Burke, and M. Ernzerhof, Phys. Rev. Lett., **77**, 3865 (1996).
[27] G. Kresse and J. Hafner, Phys. Rev. B **47**, 558 (1993); Comp. Mat. Sci. **6**, 15 (1996).
[28] M. I. Eremets, A. G. Gavriliuk, N. R. Serebryanaya, I. A. Trojan, D. A. Dzivenko, R. Boehler, H. Mao, and R. J. Hemley, J. Chem. Phys., **121**, 11296 (2004).
[29] E. Gregoryanz, A. F. Goncharov, C. Sanloup, M. Somayazulu, H. Mao, and R. J. Hemley, J. Chem. Phys., **126**, 184505 (2007).
[30] A. F. Goncharov and J. C. Crowhurst, Phys. Rev. Lett., **96**, 055504 (2006).
[31] X. Gonze, J. M. Beuken, R. Caracas, F. Detraux, M. Fuchs., G. M. Riganese, L. Sindic, M. Verstraete, G. Zerah, F. Jollet, M. Torrent, A. Roy, M. Mikami, P. Ghosez, J. Y. Raty, and D. C. Allan, Comp. Mat. Sci., **25**, 478 (2002).
[32] X. Gonze, G. M. Riganese, M. Verstraete, J. M. Beuken, Y. Pouillon, R. Caracas, F. Jollet, M. Torrent, G. Zerah, M. Mikami, P. Ghosez, M. Veithen, J. Y. Raty, V. Olevano, F. Bruneval, L. Reining, R. Godby, G. Onida, D. R. Hamann, and D. C. Allan, Zeit. Kristallogr., **220**, 558 (2005).
[33] B. Holst, R. Redmer, and M. Desjarlais, Phys. Rev. B, **77**, 184201 (2008).
[34] D. Horner, J. Kress, and L. Collins, Phys. Rev. B, **77**, 064102 (2008).
[35] A. J. Heeger, Rev. Mod. Phys., **73**, 681 (2001).
[36] M. Kertesz, C. H. Choi, and S. Yang, Chem. Rev., **105**, 3448 (2005).
[37] D. Jiang, X. Q. Chen, W. Luo, and W. A. Shelton, Chem. Phys. Lett., **483**, 120 (2009).
[38] C. Adamo and V. Barone, J. Chem. Phys., **110**, 6158 (1999).
[39] J. P. Perdew, M. Ernzerhof, and K. Burke, J. Chem. Phys., **105**, 9982 (1996).
[40] A. Pohl, H. Meider, and M. Springborg, J. Mol. Struct. (1994).
[41] P. P. Edwards and M. J. Sienko, Acc. Chem. Res., **15**, 87 (1982).